Article

Journal of
Biomedical Nanotechnology
Vol. 14, 1117–1124, 2018
www.aspbs.com/jbn

Highly Sensitive Detection of Glucose by a "Turn-Off-On" Fluorescent Probe Using Gadolinium-Doped Carbon Dots and Carbon Microparticles

Meixin Hu[1,4], Jianrong Qi[1,2], Jing Ruan[3,*], and Guangxia Shen[1,2,4,*]

[1] *Department of Instrument Science and Engineering, School of Electronic Information and Electrical Engineering, Key Laboratory for Thin Film and Microfabrication of Ministry of Education, Shanghai Jiao Tong University, Shanghai 200240, China*
[2] *State Key Laboratory of Oncogenes and Related Genes, Institute for Personalized Medicine, School of Biomedical Engineering, Shanghai Jiao Tong University, Shanghai 200030, China*
[3] *Department of Ophthalmology, Ninth People's Hospital, Shanghai Jiao Tong University School of Medicine, Shanghai 200011, China*
[4] *Shanghai Engineering Research Center for Intelligent Diagnosis and Treatment Instrument, Shanghai 200240, China*

Carbon dots, as a potential substitute for semiconductor quantum dots, have drawn great interest in recent years. The preparation of fluorescent carbon dots has been made easy with many significant advances, but the complicated purifying processes, low quantum yield, and blue emission wavelength still limit its wider application in biosensors, biomedicine, and photonic devices. Here we report a strategy to synthesis Gd-doped carbon dots (Gd-Cdots) of super-high quantum yield with a microwave assisted hydrothermal method. The Gd-Cdots, with a diameter of 4∼8 nm, can be purified easily with conventional centrifugal techniques. Carbon microparticles (CMPs) have also been synthesized with a similar procedure. Meanwhile, we demonstrated a novel "turn-off-on" fluorescent biosensor, which has been developed for highly sensitive detection of glucose using Gd-doped carbon dots as probes. The proposed biosensor has exhibited low-cost and non-toxic properties, with high sensitivity and good specificity. In addition, the results in real blood samples further confirmed it as a promising application in diabetes diagnosis.

KEYWORDS: *Gd-Doped Carbon Dots, Glucose Detection, Carbon Microparticles, Biosensors.*

INTRODUCTION

Diabetes is one of the main diseases that can significantly affect human health. Currently in the world, more than 220 million people have diabetes and the number of diabetics is growing continuously every year.[1] Therefore, it is necessary to provide more convenient and highly sensitive pre-warning and detection technologies for diabetes. Usually in clinical diagnosis, the glucose level in the blood, urine, or sweat is an important marker to measure and identify diabetes. Many glucose biosensors have been developed based on the concentration determination of blood glucose.[2–4] To date, glucose biosensors mainly include enzyme, optical, and electrochemical biosensors.[5–9] Enzyme-based biosensors are simple to use and have excellent selectivity, but it requires a long response time for detection, and its sensitivity remains to be further improved.[10–13] Optical and electrochemical detection technologies have high sensitivity but they often rely on expensive instruments.[14–17] Recently, biological detection technologies based on nanomaterials, such as semiconductor quantum dots and metallic clusters, have been extensively explored due to their special optical properties.[18–23] However, such nanomaterials utilized as fluorescent sensors are costly and toxic, which makes them unsuitable for application in real blood sample detection.[24–26]

Carbon dots (Cdots) is a type of superior fluorescent nanomaterials that exhibits good biocompatibility and high stability, and its preparation is simple and low-cost.[27,28] Compared to semiconductor quantum dots and organic fluorescent molecules, Cdots have high water solubility, chemical inertness, easy functionalization, super-high resistance to photobleaching and low toxicity.[29,30] Until

*Authors to whom correspondence should be addressed.
Emails: drjruan@163.com, gxshen@sjtu.edu.cn
Received: 17 November 2017
Accepted: 13 December 2017

now, Cdots have been widely applied in biological labeling, bioimaging, and drug delivery.[31,32] Of particular interest and significance is the recent finding where the photoluminescence (PL) of Cdots can be quenched efficiently by either electron acceptor or electron donor molecules in solution, which indicates that Cdots are excellent electron donors and electron acceptors. The particular properties further expand the application of Cdots in biological detection, light energy translation, photovoltaic devices, and related applications.[33–35] Cdots have also been used as nanoprobes for detecting DNA, metal ions, glucose, and α-fetoprotein.[36–41]

In this paper, we developed a "turn-off-on" fluorescent biosensor using Gadolinium-doped Cdots (Gd-Cdots) as probes for the detection of glucose. Gd-Cdots have been prepared *in situ* through adding Gd^{2+} ion into the reacting solution via the microwave pyrolysis approach. Then the synthesized Gd-Cdots with super-high fluorescent quantum yield (QY) were used to construct the nanoprobes to realize label-free glucose detection. In this experiment, we selected carbon microparticles (CMPs) synthesized with the microwave assisted hydrothermal method as the fluorescence quenching reagent and glucose oxidase (GOx) carries. CMPs have exhibited properties such as environmentally friendly, very low toxicity, large surface-to-volume ratio, and strong adsorption ability. Therefore, GOx can be easily loaded on the surface of CMPs through the physical adsorption process and the loading rate reached close to 100%. When Gd-Cdots met the CMPs coated with GOx (GOx@CMPs), the fluorescence of Gd-Cdots is quenched via fluorescence resonance energy transfer (FRET). Once glucose is introduced, a specific chemical reaction between GOx@CMPs and glucose induces the detaching of Gd-Cdots from the GOx@CMPs surface and thus the quenched fluorescence of Gd-Cdots was turned on again. The recovery of fluorescent intensity can be used to calculate the concentration of glucose. The selectivity and sensitivity of the fluorescent biosensor was investigated. Finally, the proposed method was successfully verified with an application of the as-prepared biosensor in real blood samples.

EXPERIMENTAL REAGENTS AND INSTRUMENTS

Materials and Instruments

Bovine serum albumin (BSA), phosphate buffer saline (PBS), cysteine, disodium hydrogen phosphate, glucose, $GdCl_3 \cdot 6H_2O$, glutathione, GOx, ascorbic acid, citric acid, strong phosphoric acid, hydrochloric acid, and tryptophan (Trp, 99%) were purchased from Sinopharm Chemical Reagent Co. Ltd. Metal ions (Fe^{3+}, Ca^{2+}, K^+, Na^+, Mg^{2+}), gadolinium chloride, monobasic, dibasic and tribasic sodium phosphates were obtained from Aladdin Chemistry Co. Ltd. All reagents used in the experiment were of analytical grades and used without further purification. All solutions were prepared using ultrapure water produced with the Millipore-Q water system.

A Jasco V-570 UV-vis spectrophotometer was used to record the UV-vis absorption spectra of the as-prepared Gd-Cdots solution, and the fluorescence spectra were captured with the F-2500 fluorescence spectrophotometer (Hitachi, Japan). The high-resolution transmission electron microscopy (HR-TEM) images were obtained using the JEOL JEM-2010 transmission electron microscope (Tokyo, Japan) with an accelerating voltage of 300 kV. Elemental and functional group analyses were acquired by a Kratos AXIS Ultra DLD X-ray photoelectron spectroscope and a PerkinElmer Paragon 1000 FTIR spectrometer, respectively.

Synthesis of Gd-Cdots and CMPs

Gd-Cdots were prepared according to our previous studies and the procedure is as follows: We mixed 0.25 g Trp, 200 mg $GdCl_3 \cdot 6H_2O$, and 0.5 g glucose into 30 mL 15% H_3PO_4 water solution. After the mixture solution became clear and homogeneous, the solution was transferred into a 50 mL poly Teflon-lined autoclave and heated at 180 °C for 20 min with the assistance of microwave radiation. The dark brown product was cooled to room temperature and dialyzed (cut of molecular weight was 1000 KD) in pure water for 48 h, and then the purified Gd-Cdots were obtained. The final transparent product was dried in a cool-vacuum desiccator for 24 h. Then the solid sample was sealed and stored in refrigerator for use at 4 °C.

The procedure for synthesizing CMPs was similar to the preparation of Gd-Cdots using microwave synthesis method. Briefly, 2 g (0.317 mol) glucose was dissolved in 25 mL ultrapure water under magnetic stirring. The obtained uniform solution was transferred into 50 mL poly Teflon-lined autoclave, and then the mixture was heated to 200 °C and kept for 20 min with the assistant of microwave radiation. After treatment, the obtained dark brown suspension was centrifuged at 5,000 rpm for 15 min to remove unreacted glucose and was washed with ethanol then water for three times. Finally, the CMPs were dried in a cool-vacuum desiccator for 24 h and collected for characterizations and further use.

Loading of GOx on CMPs

The GOx were loaded on the CMPs through the physical absorption of GOx to the surface layer of CMPs. The mass ratios of CMPs and GOx, and the loading rate have also been optimized. Various amounts of GOx ($1 \times 10^{-3} \sim 5 \times 10^{-3}$ μmol) and were separately added into 1 mL 0.1 mg/mL CMPs solution and equilibrated at 25 °C for 20 min. Then the solution was centrifuged at 8,000 rpm for 5 min and the precipitate was re-dispersed into an equal volume of sodium phosphate solution. The supernatant was also collected to calculate the uploading rate of GOx.

The final CMPs@GOx solution was kept at 4 °C prior to use.

Procedures for Detection of Glucose

The conditions for detecting glucose were optimized by varying several experimental parameters, including the pH of the solution and the concentration of CMPs@GOx. To select the appropriate pH value, aliquots of Gd-Cdots solution (0.02 mg/mL, 100 μL) were separately added to sodium phosphate solutions (1 mL, pH = 4.0–10.0) containing CMPs@GOx (GOx = 2 μM). The solutions were equilibrated at 25 °C for 20 min before PL measurements. To determine the optimal concentration of GOx, sodium phosphate solutions (1 mL, pH = 7.0) containing Gd-Cdots (0.02 mg/mL, 100 μL) and CMPs@GOx (GOx = 1–5 μM, 100 μL), they were equilibrated at 25 °C for 20 min, followed by measuring the fluorescence intensity of the solutions.

For quantitative detection of glucose, aliquots of Gd-Cdots solutions (0.02 mg/mL, 100 μL) were added to sodium phosphate solutions (1 mL, pH = 7.0) containing CMPs@GOx (GOx = 2 μM, 100 μL). After equilibrating the mixtures at 25 °C for 20 min, various amounts of glucose (0.6–40 μM, 100 μL) were added to each of the solutions. Then the mixtures were equilibrated at 25 °C for 15 min before PL measurements.

The Selectivity for Detection of Glucose

The selectivity of the proposed assay for glucose over other biological species including metal ions, thiol compounds, organic acid, and proteins was evaluated. The following possible interfering species for detection of glucose were tested: Na^+, K^+, Ca^{2+}, Mg^{2+}, glutathione, cysteine, BSA, ascorbic acid, and citric acid. The concentrations of the metal ions and organic acids were all 100 μM, and those of thiol compounds and proteins were all 10 μM. Aliquots of glucose solution (100 μM, 100 μL) mixed with these interfering species were introduced into mixtures containing Gd-Cdots (0.02 mg/mL, 100 μL) and CMPs@GOx (GOx = 2 μM, 100 μL) that had been equilibrated at 25 °C for 20 min. Subsequently, the mixtures were equilibrated at 25 °C for 15 min before PL measurements.

Detection of Glucose in Real Serum Sample

The serum sample was diluted 500 times with PBS buffer (0.1 M, pH = 7.4) and then spiked with aliquots of 0 μM, 20 μM, 30 μM, and 50 μM glucose solution. Aliquots of Gd-Cdots solution (0.02 mg/mL, 100 μL) were added to sodium phosphate solutions (1 mL, pH = 7.0) containing CMPs@GOx (GOx = 2 μM, 100 μL). Afterwards, aliquots of the diluted samples were added to the above mixture solutions and then equilibrated at 25 °C for 15 min before PL measurements.

RESULTS AND DISCUSSION

Characterization of Gd-Cdots and CMPs

Due to the super-small size of pure Cdots, the purification of Cdots was difficult. The wide distribution of Cdots would tremendously affect the QY and the emitting color of Cdots, therefore, TEM, FTIR, XPS, and fluorescence analysis were used to characterize the Gd-Cdots. Figure 1(A) displayed the TEM images of the synthesized Gd-Cdots, where we can see that these Gd-Cdots were well dispersed with good spherical morphology and the diameter of Gd-Cdots nanoparticles were between 4∼8 nm, which is larger than pure Cdots. In addition, due to doped Gadolinium, the Gd-Cdots can be easily removed from unreacted reagent by conventional centrifugation. HR-TEM image (the Zoom image of single particle, inset Fig. 1(A)) also showed that lattice finger printers were clearly observed from different direction, which pointed that the Gd-Cdots has good crystal and graphene structure. The UV-vis absorption spectra and PL spectrum of the Gd-Cdots were presented in Figure 1(B). The UV-vis spectra exhibited two absorption peaks at the wavelengths around 237 nm and 332 nm. The peak at 237 nm was attributed to the π–π^* transition of the conjugated C═C structure and the absorption peak at 332 nm corresponded to the n–π^* of the C═O transition. So it can emit bring blue light with a 365 nm UV lamp (see inset Fig. 1(B)). Meanwhile, the fluorescence emission peak was recorded at around 445 nm upon excitation at 365 nm in Figure 1(B). The emission wavelength and intensity changed with the excitation wavelength and have the strongest intensity at 445 nm with excitation at 365 nm. By controlling the reacting condition (reacting time, mass ratio, microwave power and temperature), we can obtain different FL of Gd-Cdots. The FTIR spectra represented in Figure 1(C) showed a couple of vibration bands. The peaks at 1635 and 1203 cm^{-1} could be attributed to the plane bending vibrations of C═C and C–O–C, respectively. The peak around 3408 cm^{-1} corresponded to the vibrations of O–H or N–H bonds. The XPS survey of the Gd-Cdots in Figure 1(D) showed three predominant peaks at 284.7 eV, 398.7 eV, and 531.2 eV, which corresponds to C1s, N1s and O1s respectively. It indicates that the synthesized Gd-Cdots are mainly consisted of four major elements, C, N, O and Gd.

Figure 2(A) is the TEM image of the CMPs that were synthesized via the microwave-assisted hydrothermal method. The TEM results showed a good spherical shape with an average diameter of about 100∼200 nm. From the HR-TEM in Figure 2(B), we can see the fine structure of the CMPs. The CMPs surface was crude and wrapped by organic coatings. The UV-vis. absorption spectrum in Figure 2(C) shows a sharp peak at 280 nm corresponding to the sp^2 carbon core and π–π^* transition of the C═C structure. Furthermore, Figure 2(D) exhibits the FTIR spectra of CMPs, which shows that the elasticity vibration of O–H is at 3408 cm^{-1}, and the plane

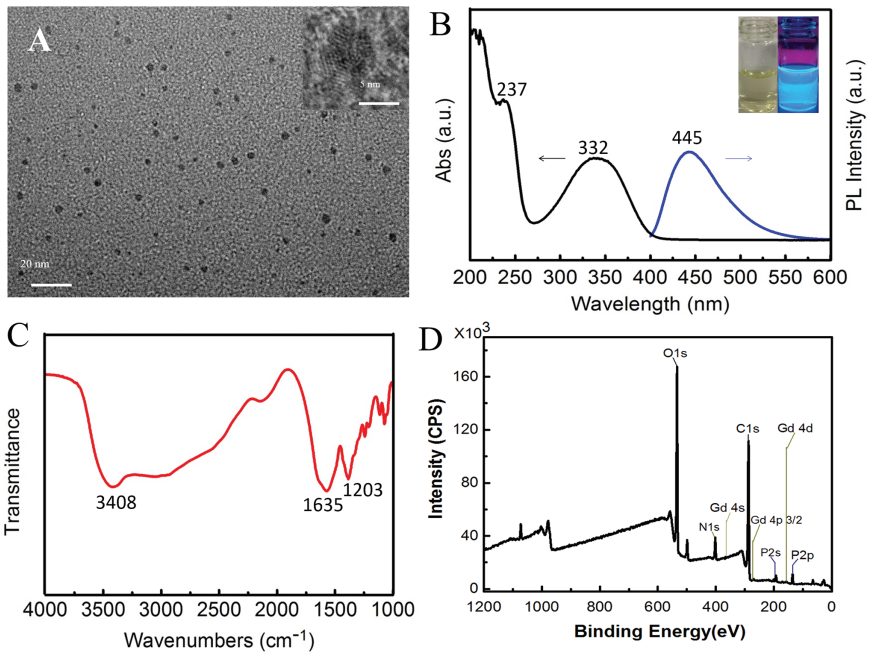

Figure 1. **(A) HR-TEM images of the Gd-Cdots; (B) UV-vis absorption (black line) and photoluminescence spectrum (blue line, excitation at 365 nm) of Gd-Cdots. Inset: Photographs of Gd-Cdots solution under daylight (left) and UV lamp (right, 365 nm). (C) FTIR spectrum of the Gd-Cdots. (D) XPS survey spectrum of the Gd-Cdots.**

bending vibrations of C═O and C–O–C is at 1635 cm^{-1} and 1350 cm^{-1}, respectively.

Detection Mechanism of the Gd-Cdots Probes

Scheme 1 illustrated the sensing strategy for glucose detection of the as-prepared biosensor. Due to the peculiar properties of Cdots as a perfect electron acceptor and electron donor molecules in solution, Cdots have been widely applied in biological detection and biosensors. In the detection process, GOx was first modified on the surface of CMPs through physical absorption due to the high surface energy and lager specific surface area. Then after the

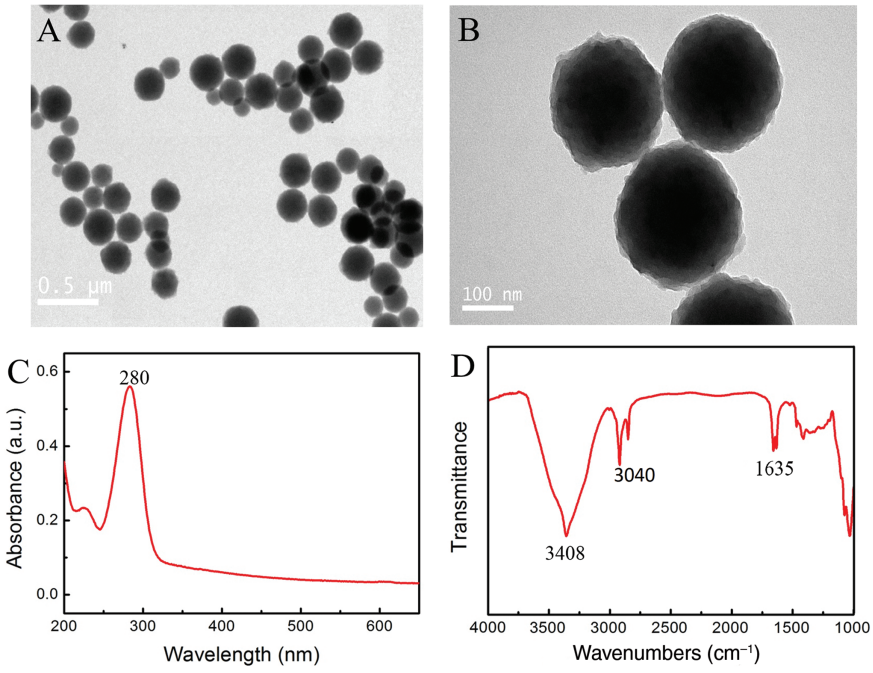

Figure 2. **(A, B) TEM and HR-TEM images of carbon microspheres (CMPs); (C) UV-vis. absorption of CMPs; (D) FTIR spectrum of the CMPs.**

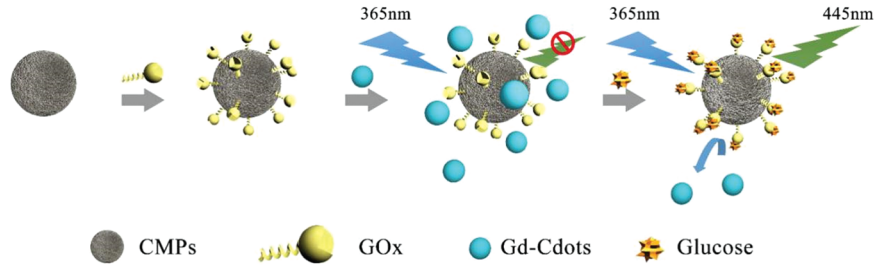

Scheme 1. **The detection mechanism based on FRET between the Gd-Cdots and CMPs@GOx for glucose.**

CMPs@GOx nanoparticles adding into the Gd-Cdots solution, the fluorescence of Gd-Cdots was quickly "turned off" due to fluorescence resonance energy transfer (FRET). It can be explained by a π–π bond interaction when Gd-Cdots were very close to the CMPs@GOx particles. Once glucose was introduced into the solution, the small molecules of glucose inset into the space between CMPs@GOx particles and Gd-Cdots. Glucose preferentially reacted with GOx on the surface of CMPs, and the Gd-Cdots were crowded out and the fluorescence was "turned on" again. The recovery rate of fluorescence intensity positively correlated with the concentration of glucose that was added.

Optimization of the Assay Conditions

Before the detection of glucose, we have systematically investigated the loading rate of GOx on the CMPs surface, and the effects of pH and the concentration of GOx@CMPs on the fluorescence properties of the Gd-Cdots. Due to super-high surface-to-volume ratio, the CMPs as-synthesized can quickly and strongly absorb GOx on the surface within 20 min under mild conditions by physical absorption process. The loading rate reached near to 100% by comparing the UV-vis. absorption values of GOx before and after the physical interaction as shown in Figure 3(A). And in this process we dropped 2×10^{-3} μmol GOx into 0.1 mL^{-1} mg/mL CMPs water solution under mild string without heated or other harsh conditions. And the evolvement of GOx loaded onto the surface of CMPs have monitored by testing UV-Absorption spectra every five minutes. In Figure 3(B), the results have shown GOx can be completely absorbed onto the surface of CMPs in 20 min. And so in our experiments we used the loading time of 20 min unless specifically specified.

In addition, the concentration of the CMPs@GOx plays a key role. Therefore, we have primarily inspected the concentration influence of the CMPs@GOx on fluorescence quenching of Gd-Cdots. As shown in Figure 4(A), by increasing the concentration of CMPs@GOx, the FL of the Gd-Cdots solution was quenched, and the maximum ΔF was obtained when the concentration of CMPs@GOx increased to 2 μM. Here, ΔF stands for the absolute value of FL intensity change of the Gd-Cdots solution in the absence and presence of 2 μM CMPs@GOx. We speculated that in the lower concentration of CMPs@GOx (<2 μM), the CMPs@GOx particles will be single dispersed in the solution and the rate of random collision increases with the increase of CMPs@GOx concentration. However, with the increase of CMPs@GOx concentration, the microparticles themselves will aggregate, which caused the ΔF value to decrease. As a result, 2 μM CMPs@GOx was selected as the optimal concentration for the detection.

In addition, the pH value is another important factor that affects the interaction between Gd-Cdots and CMPs@GOx. As we know, the distance of Gd-Cdots and CMPs@GOx gets much closer if there is much stronger interaction between them. In view of practical application, we inspected the pH of Gd-Cdots solution at a range of 4.0~10.0 in the mixture solution of 2 μM CMPs@GOx and 0.02 mg/mL Gd-Cdots (shown in Fig. 4(B)). The results have showed the FL intensity has still kept high

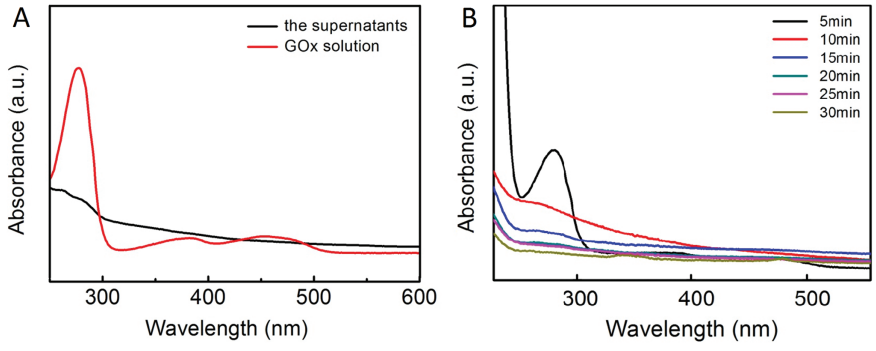

Figure 3. **(A) UV-absorption spectra of GOx before or after being added CMPs following centrifugal treatment; (B) UV-absorption spectra *in situ* recording the loading process of GOx on the CMPs surface.**

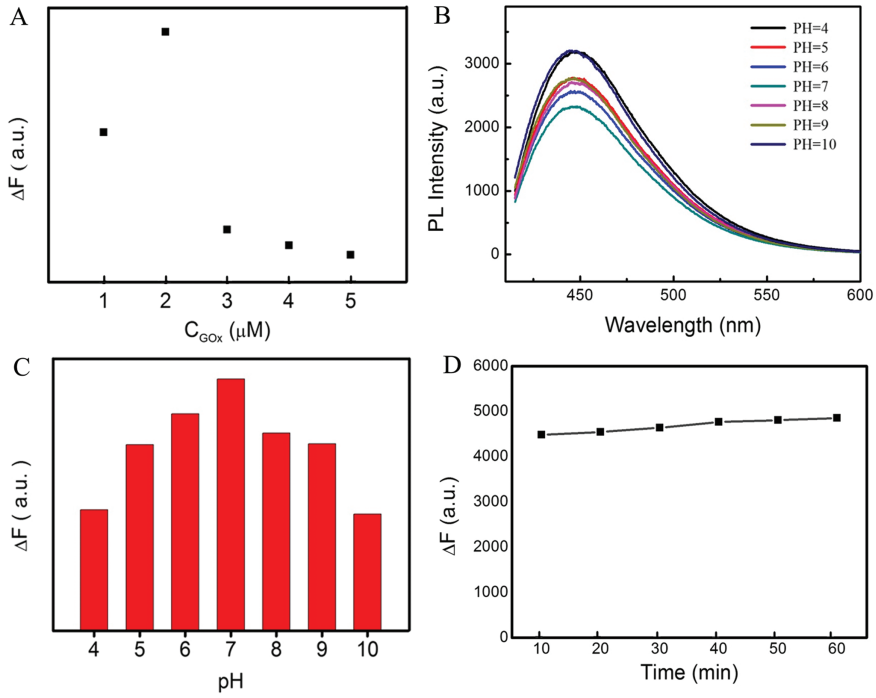

Figure 4. **(A) Optimizing GOx concentration by monitoring influence of the CMPs@GOx concentration (GOx, 1–5 μM) on ΔF; (B) PL spectra changes of the 0.02 mg/mL Gd-Cdots and 2 μM CMPs@GOx mixture solution with variation of pH by adding diluted HCl or NaOH; (C) Histogram of pH (4.0–10.0) versus ΔF intuitively pointing to the pH influences on the detecting system; (D) the plot of ΔF with time delay in PBS buffer (pH = 7.0) solution. ΔF is the absolute change of PL intensities of the solutions in the absence and presence of CMPs@GOx.**

value at pH 4 or pH 10, and significantly decreased at pH 7 in the mixture solution of 2 μM CMPs@GOx and 0.02 mg/mL Gd-Cdots. From Figure 4(C), we could intuitively see the variation of the ΔF value with the different pH. At pH 7, the ΔF reached the largest, thus it can ensure the widest detecting range of the detection system. Simultaneously, we also investigated the stability of the ΔF value with time delay at pH 7 solution in

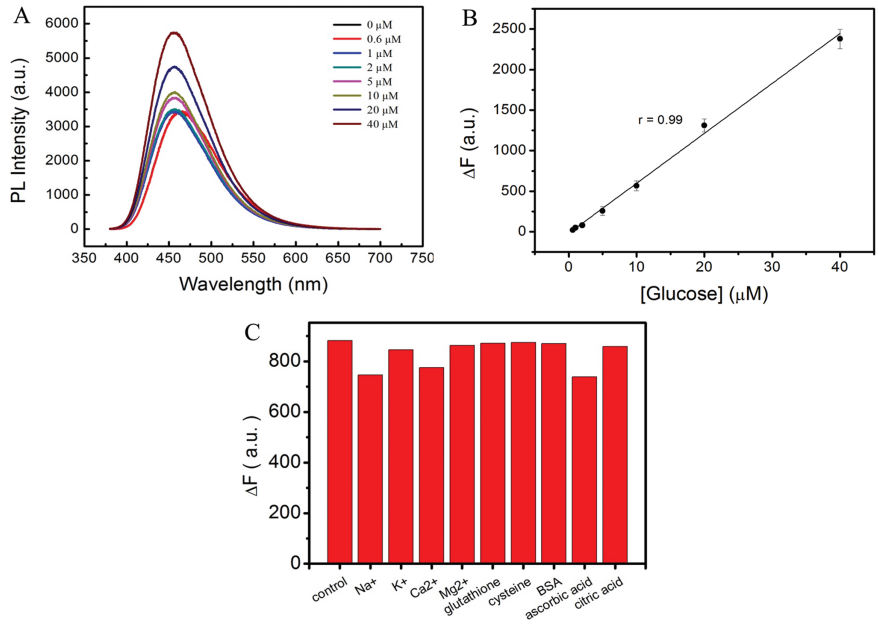

Figure 5. **(A) FL spectras of the mixture solution with adding different concentration of glucose; (B) calibration plots of ΔF versus the concentration of glucose. (C) Selectivity of the assay towards glucose (100 μM) in the presence of other potential interfering species. Excitation and emission wavelengths are 365 and 445 nm, respectively.**

Figure 4(D). The results exhibited ΔF had no significant change in the range of 10~60 minutes. Hence, the pH value of 7.0 was used as the optimal condition.

Glucose Detection with the Gd-Cdots-Based Bioprobes

Under the optimized conditions, we used 2 μM CMPs@GOx to add into 2 μM Gd-Cdots solution as detection system and the ΔF for various concentrations of glucose were recorded. The FL of the solution would be recovered with the addition of glucose as shown in Figure 5(A). Meanwhile, a calibration curve was constructed by plotting the fluorescence quenching ΔF versus the concentration of glucose. It can be seen from Figure 5(B) that the resulting curve had good linearity for glucose concentration range of 0.6–40.0 μM, with a correlation coefficient of 0.9912. The detection limit was as low as 0.6 μM, which compares favorably with other reported methods' results.[42–46]

The Selectivity for Detection of Glucose

The detection selectivity has been investigated, and its effects of other biological species on the detection of glucose through the proposed bioprobes. Figure 4(C) showed the fluorescence quenching ΔF of the Gd-Cdots solution in the presence of 100 μM glucose and other interfering species with concentrations of 100 μM or 10 μM. From Figure 5(C) we find that there is no obvious interference effect on the result when in co-existence of the interfering substance, in comparison with the pure glucose detection. It proved that the Gd-Cdots-based biosensor was highly selective towards glucose over other species. This finding also suggests the potential as a biosensor for glucose detection in blood samples.

Analysis of Blood Samples

To evaluate the practical feasibility of the proposed biosensor, the standard recovery experiments were performed to detect the concentration of glucose in real human serum samples. The obtained results were summarized in Table I. The recoveries of all samples were in the range of 90.5%~106.5%, proving the precision and reliability of the present method for the detection of glucose in practical samples.

Table I. Determination and recovery tests of glucose in real human serum samples using the proposed biosensor.

Sample	Added (μM)	Found (μM)[b]	Recovery (%, $n = 3$)	RSD (%, $n = 3$)
Human serum[a]	0	10.65	106.5	2.7
	20	13.58	90.5	3.9
	30	21.09	105.5	3.0
	50	30.19	100.6	2.8

Notes: [a]Reference value (determined by hospital) = 5.00 mM; [b]calculate value considering dilution factor (500-fold), 10.65 × 500 = 5.325 mM.

CONCLUSIONS

In summary, we used a facile method to synthesis Gd-doped Cdots of super-high quantum yield and CMPs with microwave assisted hydrothermal methods. The two types of materials are derived from glucose, but have completely different properties based on preparation condition. They have low-toxicity and are environmentally friendly. Based on their distinct properties, the novel "turn-off-on" fluorescent biosensor using Gd-doped carbon dots as probes has been utilized for highly sensitive detection of glucose. In the detection system, we found that the recovery rate of fluorescence is proportional to the amount of glucose present, and the detection sensitivity can be as low as 0.6 μM in view of practical applications. The proposed biosensor exhibits several advantages, including low-cost, non-toxic, high sensitivity, and good specificity. In addition, it was applied for the determination of glucose in real blood samples with satisfactory results, indicating it as a promising application in diabetes diagnosis.

Acknowledgments: We are gratefully to Professor Kong Xiangyang for providing experimental instructions and testing instruments to us. The work was supported by the National Natural Science Foundation of China (Grant Nos. 31170961, 31771088, 81601623); Biomedical and Engineering Multidisciplinary Funding of SJTU (Nos. YG2016MS03 and G2014MS01); Shanghai Rising-Star Program (17QA1402000). We would also like to thank Instrumental Analysis Center of SJTU for the TEM, FTIR and XPS analysis measurements.

REFERENCES

1. J. E. Shaw, R. A. Sicree, and P. Z. Zimmet, Global estimates of the prevalence of diabetes for 2010 and 2030. *Diabetes Res. Clin. Pract.* 87, 4 (**2010**).
2. L. Shang, Y. Cheng, and Y. Zhao, Emerging droplet microfluidics. *Chem. Rev.* 117, 7964 (**2017**).
3. Y. Zhao, Y. Cheng, L. Shang, J. Wang, Z. Xie, and Z. Gu, Microfluidic synthesis of barcode particles for multiplex assays. *Small* 11, 151 (**2015**).
4. L. Shang, F. Fu, Y. Cheng, H. Wang, Y. Liu, Y. Zhao, and Z. Gu, Photonic crystal microbubbles as suspension barcodes. *J. Am. Chem. Soc.* 137, 15533 (**2015**).
5. X. Y. Huang and J. C. Ren, Nanomaterial-based chemiluminescence resonance energy transfer: A strategy to develop new analytical methods. *Trac.-Trend Anal. Chem.* 40, 77 (**2012**).
6. T. Lenarczuk, D. Wencel, S. Głąb, and R. Koncki, Prussian blue-based optical glucose biosensor in flow-injection analysis. *Anal. Chim. Acta* 447, 23 (**2001**).
7. P. Roy, Z. H. Lin, C. T. Liang, and H. T. Chang, Synthesis of enzyme mimics of iron telluride nanorods for the detection of glucose. *Chem. Commun. (Camb.)* 48, 4079 (**2012**).
8. Y. C. Shi, C. C. Huang, and H. T. Chang, Gold nanodot-based luminescent sensor for the detection of hydrogen peroxide and glucose. *Chem. Commun. (Camb.)* 23, 3437 (**2009**).
9. D. L. Williams, A. R. Doig, and A. Korosi, Electrochemical-enzymatic analysis of blood glucose and lactate. *Anal. Chem.* 42, 118 (**1970**).

10. M. Gu, J. Wang, Y. Tu, and J. Di, Fabrication of reagentless glucose biosensors: A comparison of mono-enzyme GOD and bienzyme GOD-HRP systems. *Sens. Actuat. B-Chem.* 148, 486 **(2010)**.

11. F. X. Qin, S. Y. Jia, F. F. Wang, S. H. Wu, J. Song, and Y. Liu, Hemin@metal-organic framework with peroxidase-like activity and its application to glucose detection. *Catal. Sci. Technol.* 3, 2761 **(2013)**.

12. Q. Chen, M. Liu, J. Zhao, X. Peng, X. Chen, N. Mi, B. Yin, H. Li, Y. Zhang, and S. Yao, Water-dispersible silicon dots as a peroxidase mimetic for the highly-sensitive colorimetric detection of glucose. *Chem. Commun.* 50, 6771 **(2014)**.

13. W. Zhang, D. Ma, and J. Du, Prussian blue nanoparticles as peroxidase mimetics for sensitive colorimetric detection of hydrogen peroxide and glucose. *Talanta* 120, 362 **(2014)**.

14. E. Go, H. Kim, and C. Kim, Synthesis of one-dimensional pillar arrays by electrohydrodynamic jet printing for glucose sensor. *J. Biomed. Nanotechnol.* 13, 61 **(2017)**.

15. J. Liu, Y. Luo, Y. Wang, L. Duan, J. Jiang, and R. Yu, Graphitic carbon nitride nanosheets-based ratiometric fluorescent probe for highly sensitive detection of H_2O_2 and glucose. *ACS Appl. Mater. Interfaces* 8, 33439 **(2016)**.

16. L. Han, C. Shao, B. Liang, and A. Liu, Genetically engineered phage-templated MnO_2 nanowires: Synthesis and their application in electrochemical glucose biosensor operated at neutral pH condition. *ACS Appl. Mater. Interfaces* 8, 13768 **(2016)**.

17. X. Du, Y. Li, J. R. Motley, W. F. Stickle, and G. S. Herman, Glucose sensing using functionalized amorphous In–Ga–Zn–O field-effect transistors. *ACS Appl. Mater. Interfaces* 8, 7631 **(2016)**.

18. Y. Miao, J. Zhao, H. He, Y. Du, Y. Liu, and P. Yang, Attachment of hybrid SiO_2 coated CdTe quantum dots to graphene for ion sensors. *J. Nanosci. Nanotechnol.* 16, 9806 **(2016)**.

19. Y. He, X. Wang, J. Sun, S. Jiao, H. Chen, F. Gao, and L. Wang, Fluorescent blood glucose monitor by hemin-functionalized graphene quantum dots based sensing system. *Anal. Chim. Acta* 810, 71 **(2014)**.

20. G. Wen, P. Wang, W. Tu, J. Lei, and H. Ju, Biosensing strategy based on photocurrent quenching of quantum dots via energy resonance absorption. *Sci. China Chem.* 58, 879 **(2015)**.

21. M. Hu, J. Tian, H. T. Lu, L. X. Weng, and L. H. Wang, H_2O_2-sensitive quantum dots for the label-free detection of glucose. *Talanta* 82, 997 **(2010)**.

22. Y. C. Shiang, C. C. Huang, and H. T. Chang, Gold nanodot-based luminescent sensor for the detection of hydrogen peroxide and glucose. *Chem. Commun.* 23, 3437 **(2009)**.

23. Y. Ling, N. Zhang, F. Qu, T. Wen, Z. F. Gao, N. B. Li, and H. Q. Luo, Fluorescent detection of hydrogen peroxide and glucose with polyethyleneimine-templated Cu nanoclusters. *Spectrochim. Acta A* 118, 315 **(2014)**.

24. J. Lovrić, S. J. Cho, F. M. Winnik, and D. Maysinger, Unmodified cadmium telluride quantum dots induce reactive oxygen species formation leading to multiple organelle damage and cell death. *Chem. Biol.* 12, 1227 **(2005)**.

25. Y. Su, M. Hu, C. Fan, Y. He, Q. Li, W. Li, L. Wang, P. Shen, and Q. Huang, The cytotoxicity of CdTe quantum dots and the relative contributions from released cadmium ions and nanoparticle properties. *Biomaterial* 31, 4829 **(2010)**.

26. N. Chen, Y. He, Y. Su, X. Li, Q. Huang, H. Wang, X. Zhang, R. Tai, and C. Fan, The cytotoxicity of cadmium-based quantum dots. *Biomater.* 33, 1238 **(2012)**.

27. C. Savita, A. Umar, and K. K. Bhasin, Applications of carbon dots in nanomedicine. *J. Biomed. Nanotechnol.* 13, 591 **(2017)**.

28. L. C. Ingeborg and Y. P. Sun, Carbon dots as antioxidants and prooxidants. *J. Biomed. Nanotechnol.* 7, 667 **(2011)**.

29. K. Wang, Z. Gao, G. Gao, Y. Wo, Y. Wang, G. Shen, and D. Cui, Systematic safety evaluation on photoluminescent carbon dots. *Nanoscale Res. Lett.* 8, 122 **(2013)**.

30. Z. Gao, G. Shen, X. Zhao, N. Dong, P. Jia, J. Wu, D. Cui, Y. Zhang, and Y. Wang, Carbon dots: A safe nanoscale substance for the immunologic system of mice. *Nanoscale Res Lett.* 8, 276 **(2013)**.

31. N. Durán, M. B. Simões, A. C. M. de Moraes, W. J. Fávaro, and A. B. Seabra, Nanobiotechnology of carbon dots: A review. *J. Biomed. Nanotechnol.* 12, 1323 **(2016)**.

32. S. Chaudhary, A. Umar, K. K. Bhasin, and S. Singh, Applications of carbon dots in nanomedicine. *J. Biomed. Nanotechnol.* 13, 591 **(2017)**.

33. J. F. Fong, S. F. Chin, and S. M. Ng, A unique "turn-on" fluorescence signaling strategy for highly specific detection of ascorbic acid using carbon dots as sensing probe. *Biosens. Bioelectron.* 85, 844 **(2016)**.

34. K. Qu, J. Wang, J. Ren, and X. Qu, Carbon dots prepared by hydrothermal treatment of dopamine as an effective fluorescent sensing platform for the label-free detection of iron (III) ions and dopamine. *Chemistry* 19, 7243 **(2013)**.

35. Z. Fu, M. Yao, X. Niu, and F. Cui, Facile synthesis of highly luminescent co-doped carbon nanodots for rapid, sensitive, and label-free detection of Hg^{2+}. *Sens. Actuat. B-Chem.* 226, 486 **(2016)**.

36. H. Miao, L. Wang, Y. Zhuo, Z. Zhou, and X. Yang, Label-free fluorimetric detection of CEA using carbon dots derived from tomato juice. *Biosens. Bioelectron.* 86, 83 **(2016)**.

37. H. M. Goncalves, A. J. Duarte, and J. C. Esteves da Silva, Optical fiber sensor for Hg(II) based on carbon dots. *Biosens. Bioelectron.* 26, 1302 **(2010)**.

38. S. Chandra, D. Laha, A. Pramanik, A. Ray Chowdhuri, P. Karmakar, and S. Kumar Sahu, Synthesis of highly fluorescent nitrogen and phosphorus doped carbon dots for the detection of Fe (3+) ions in cancer cells. *Luminescence* 31, 81 **(2016)**.

39. X. Zhang, C. Liu, Z. Li, J. Guo, and L. Shen, An easily prepared carbon quantum dots and employment for inverted organic photovoltaic devices. *Chem. Eng. J.* 315, 621 **(2017)**.

40. X. Yu, R. Liu, G. Zhang, and H. Cao, Carbon quantum dots as novel sensitizers for photoelectrochemical solar hydrogen generation and their size-dependent effect. *Nanotechnology* 24, 335401 **(2013)**.

41. S. Paulo, E. Palomares, and E. Martinez-Ferrero, Graphene and carbon quantum dot-based materials in photovoltaic devices: From synthesis to applications. *Nanomaterials* 6, 157 **(2016)**.

42. Y. G. Zhou, S. Yang, Q. Y. Qian, and X. H. Xia, Gold nanoparticles integrated in a nanotube array for electrochemical detection of glucose. *Electrochem. Commun.* 11, 216 **(2009)**.

43. G. Wang, N. M. Thai, and S. T. Yau, Preserved enzymatic activity of glucose oxidase immobilized on unmodified electrodes for glucose detection. *Biosens. Bioelectron.* 22, 2158 **(2007)**.

44. B. Tang, L. Cao, K. Xu, L. Zhuo, J. Ge, Q. Li, and L. Yu, A new nanobiosensor for glucose with high sensitivity and selectivity in serum based on fluorescence resonance energy transfer (FRET) between CdTe quantum dots and Au nanoparticles. *Chemistry* 14, 3637 **(2008)**.

45. W. B. Shi, Q. Wang, Y. Long, Y. Cheng, S. Chen, H. Zheng, and Y. Huang, Carbon nanodots as peroxidase mimetics and their applications to glucose detection. *Chem. Commun.* 47, 6695 **(2011)**.

46. H. Wei and E. Wang, Fe_3O_4 magnetic nanoparticles as peroxidase mimetics and their applications in H_2O_2 and glucose detection. *Anal. Chem.* 80, 2250 **(2008)**.